Talanta 98 (2012) 172–177

Contents lists available at SciVerse ScienceDirect

Talanta

journal homepage: www.elsevier.com/locate/talanta

Non-destructive crystal size determination in geological samples of archaeological use by means of infrared spectroscopy

M. Olivares [a,*], A. Larrañaga [b], M. Irazola [a], A. Sarmiento [a], X. Murelaga [c], N. Etxebarria [a]

[a] University of the Basque Country, Faculty of Science and Technology, Department of Analytical Chemistry, P.O. Box 644 E-48080, Bilbao, Basque Country, Spain
[b] University of the Basque Country, Faculty of Science and Technology, General Research Services (SGIker), P.O. Box 644 E-48080, Bilbao, Basque Country, Spain
[c] University of the Basque Country, Faculty of Science and Technology, Department of Stratigraphy and Paleontology, P.O. Box 644 E-48080, Bilbao, Basque Country, Spain

ARTICLE INFO

Article history:
Received 8 March 2012
Received in revised form
18 June 2012
Accepted 25 June 2012
Available online 29 June 2012

Keywords:
Crystal size
X-ray diffraction
Infrared spectroscopy
Partial least square regression
Archeological samples

ABSTRACT

The determination of crystal size of chert samples can provide suitable information about the raw material used for the manufacture of archeological items. X-ray diffraction (XRD) has been widely used for this purpose in several scientific areas. However, the historical value of archeological pieces makes this procedure sometimes unfeasible and thus, non-invasive new analytical approaches are required. In this sense, a new method was developed relating the crystal size obtained by means of XRD and infrared spectroscopy (IR) using partial least squares regression. The IR spectra collected from a large amount of different geological chert samples of archeological use were pre-processed following different treatments (i.e., derivatization or sample-wise normalization) to obtain the best regression model. The full cross-validation was satisfactorily validated using real samples and the experimental root mean standard error of precision value was 165 Å whereas the average precision of the estimated size value was 3%. The features of infrared bands were also evaluated in order to know the background of the prediction ability. In the studied case, the variance in the model was associated to the differences in the characteristic stretching and bending infrared bands of SiO_2. Based on this fact, it would be feasible to estimate the crystal size if it is built beforehand a chemometric model relating the size measured by standard methods and the IR spectra.

1. Introduction

Flint has been widely used during prehistoric times and questions about the sources and origins of specific artefacts are recurrent in archeological discussions. Determining the origins of lithic raw material is one of the keys to resolve those questions and to infer some observed behaviors in ancient human populations [1]. In this framework, the analysis of the morphological and compositional information provides some insights about the sedimentary environment of the raw material, giving clues about some of the answers we are looking for. However, subtle variations in chemical and mineralogical characteristics might have had enough weight to vary chert's value from an archeological point of view. One of these features is the mechanical properties of knappable toolstones that have been widely studied by archaeologists to understand the knapping techniques [2].

Ethnographic and archeological evidences have revealed that, in many of the prehistoric societies, certain knappable siliceous rocks were often deliberately heated to improve their flaking properties. Every source raw material may respond slightly different, when they are exposed to heat (between 200 and 450 °C), based on their composition or specimen size. In this sense, archeologists sought different successful heat treatment strategies in order to understand whether ancient knappers could have improved their raw material with heat [3].

The subsequent concern will be how to detect heat treatment in archeological items. Leaving aside the use of thermal luminescence to date heat treatments with flint samples [4,5], the study of changes in the color or increased greasy luster or the subtle change in the magnetic susceptibility in thermally altered artefacts are some reliable fast methods for identifying heat treatment procedures [6,7].

Additionally, it has been demonstrated that heat treatment of flint up to 400 °C causes re-crystallization of quartz crystals (i.e., large numbers of smaller, poorly ordered and thermodynamically unstable crystals grow into fewer, larger and better ordered crystals) which depends on the silica phase and size of quartz crystals [8]. The heated re-crystallized flint samples are therefore structurally different to the original materials, and will respond differently to fracture propagation. That is, fracturing within microcrystalline quartz occurs along crystal boundaries rather than through crystals because the bonding between crystals is

* Corresponding author. Tel.: +34 946 015 551; fax: +34 946 013 500.
E-mail address: maitane.olivares@ehu.es (M. Olivares).

0039-9140/$ - see front matter © 2012 Elsevier B.V. All rights reserved.
http://dx.doi.org/10.1016/j.talanta.2012.06.066

much weaker than the stronger interatomic silicon–oxygen bonds within the crystals. The shape and size of individual quartz crystals will therefore determine fracture propagation. Thus, those flints having larger quartz crystals initially or after heating treatments will present better knapping properties [9,10]. The efforts to understand what is behind the improvement of lithic materials properties are evidenced in the literature. Although several models of the structural transformations upon heating have been proposed during years, new proposals involving infrared spectroscopy, solid state NMR, X-ray diffraction and electron microscopy are currently in vogue [11–13].

The estimation of quartz crystal size can be therefore an effective procedure to predict the suitability of the siliceous rock for archeological purposes. Owing to this requirement, Scanning Electron Microscopy (SEM) and, above all, X-ray Diffraction (XRD) have been widely used to determine crystal size [14]. Traditionally, the crystal size can be determined accurately based on the peak width of the principal XRD peak using Scherrer formula [15], as shown in Eq. (1):

$$\beta_{hkl} = 0.89 \cdot \lambda / L_{hkl} \cdot \cos\theta \quad (1)$$

from which the well-known Bragg equation can be developed, where β_{hkl} is the broadening of the diffraction line measured at half the line maximum intensity (FWHM), λ is the X-ray wavelength, L_{hkl} is the crystal size and θ is the diffraction angle. The broadening of the peak is related to the crystal size and to the wavelength provided by the equipment used. Typically, the peak is not a line but an interval and the Bragg β_{hkl} can be shown in Eq. (2):

$$\beta_{hkl} = (B_{hkl} - b) \quad (2)$$

where B_{hkl} is the broadening measured on the X-ray pattern and b is the unavoidable broadening of the equipment that can be determined with a standard of LaB_6.

XRD analyses require special care (i.e. homogeneous small particle size materials) which means, in most of the cases, the destruction of the archeological sample. However, due to the historical and archeological value of some flint samples, alternative non-destructive ways to estimate the crystal size would be acknowledged. Owing to these requirements vibrational spectroscopic techniques show promising features to undertake non-destructive crystal size measurements. In fact, Raman spectroscopy coupled to Scanning Electron Microscopy has been used to get molecular information and to associate this with the variation of the crystal size [16]. Infrared spectroscopy is another alternative and precisely the main aim of this work was to explore the feasibility of infrared spectra to estimate the crystal size using geological chert samples that are known to be of archeological interest.

2. Experimental

2.1. Samples

In the Basque Cantabrian region a high variety of silicifications can be found according to the age formation (Jurassic, Early and Late Cretaceous, Paleocene, Eocene and Miocene periods) and also to the formation environments (deep seabeds, ocean shelves, reefs and continental contexts). Due to that, the crystal size determination was carried out using chert samples and 65 samples from 14 different geological settings were collected along the Basque–Cantabrian region in order to get all the major representativeness of this type of samples. Regarding to the sample pre-treatment, since the IR measurements were accomplished by Attenuated Total Reflectance (ATR-IR), no special sample pre-treatment was required. One of the inconvenience that arises from the use of ATR-IR equipments is that total contact of the sample surface and ATR crystal must be guaranteed in order to obtain reliable spectra. Because of both the small size and the flat surfaces of the analyzed samples, an efficient contact with the ATR crystal was possible. In the case of XRD analyses, all the samples were ground in an agate ball-mill (Pulverissette, Frisch, Germany) to make the power diffraction measurements.

2.2. X-ray diffraction measurements

The crystal size determination was carried out by the standardized quantitative method, which is accomplished by means of X-ray diffraction and using Scherrer formula. The XRD data collected at room temperature were carried out on a High Resolution Bruker D8 Advance diffractometer equipped with a Cu tube, Ge(111) incident beam monochromator ($\lambda = 1.5406$ Å) and a Sol-X energy dispersive detector. The samples were mounted on a zero background silicon wafer embedded in a generic sample holder. Data were collected from 25° to 28° 2θ (step size = 0.01 and time per step = 25 s) at room temperature (RT). A fixed divergence and antiscattering slit of 1° giving a constant volume of sample illumination were used.

2.3. Infrared spectroscopy measurements

The infrared equipment used in this work was Jasco-6300 spectrometer (Jasco, Japan). Unlike measures in transmittance mode, reflectance measures allow acquiring the infrared spectra directly without any pre-treatment of the sample. Thus, all infrared spectra collected in this work have been carried out in total reflectance mode by attaching an attenuated total reflectance (ATR-IR) module (Single reflection ATR, Miracle, Pike, USA). The measurements were performed using a single-reflection sampling plate with a 1.8 mm round crystal (diamond/ZnSe) surface allowing reliable analysis of small samples. The module is provided with a high-pressure rotating clamp which is calibrated to deliver over 10,000 psi. All the measurements were carried out in the same pressure conditions which were controlled by the specifications of the equipment. The infrared spectra were collected in the mid-infrared region from 4000 cm^{-1} to 600 cm^{-1} with a spectral resolution of 4 cm^{-1} and accumulating 40 scans during 4 s in each spectrum to get a good signal to noise ratio. The representativeness of the obtained spectra was guaranteed by taking three spectra per sample and analyzing more than three samples per type of chert (see Table 1).The instrument is controlled by Jasco software that also allows processing the IR spectra.

3. Results and discussion

3.1. Determination of crystal size by means of XRD

Particle size determination was performed accurately by means of XRD and using Scherrer formula (see Eq. 1) which provides for particle sizes lower than 1000 Å a standard deviation of less than 5%. Peak shapes were fitted by convolution of a Scherrer-type broadening term of form (λ/size)cos θ with an instrumental resolution function derived from a highly crystalline LaB_6 standard recorded under equivalent conditions. The information from broadened X-ray diffraction lines is normally used to estimate average crystal size defined as average domain size (D) by Scherrer equation ($k = 0.9$, $\beta_{Inst} = 0.05°$). In order to calculate the crystallite sizes of the α-quartz samples the diffraction line widths of the observed (101) reflections were measured. In this

Table 1
Crystal size of some chert samples determined by means of XRD and the use of Scherrer formula.

Geological setting	*Geological time and context*	*Sample name*	*FWHM 2θ*	*Crystallite size* (Å)	*Geological setting*	*Geological time and context*	*Sample name*	*FWHM 2θ°*	*Crystallite size* (Å)
Ablitas (*ABL*, *Navarre*)	Miocene lacustrine	ABL1	0,167	**700**	*Cucho silcrete* (*CU*, *Burgos*)	Miocene lacustrine	CU1	0,182	**620**
		ABL1	0,123	**1120**			CU2	0,200	**545**
		ABL2	0,163	**720**			CU3	0,193	**570**
		ABL4	0,126	**1075**			CU7	0,165	**710**
Tobera (*TOB*, *Alava*)	Eocene lacustrine	TOB3	0,154	**785**			CU8	0,178	**640**
		TOB4	0,165	**710**			CU9	0,175	**650**
		TOB5	0,164	**720**			CU10	0,190	**580**
Artxilondo (*ARTX*, *Navarre*)	Paleocene abyssal plain	ARTX2	0,128	**1050**	*Cucho laminar* (*CU*, *Burgos*)	Miocene lacustrine	CU4	0,172	**670**
		ARTX3	0,110	**1360**			CU5	0,194	**565**
		ARTX4	0,111	**1340**			CU6	0,180	**630**
		ARTX5	0,134	**970**	*Cucho nodular* (*CU*, *Burgos*)	Miocene lacustrine	CU11	0,230	**455**
		ARTX5	0,122	**1135**			CU12	0,217	**490**
		ARTX6	0,164	**715**			CU13	0,216	**490**
		ARTX7	0,140	**910**			CU14	0,222	**475**
		ARTX8	0,119	**1185**			CU15	0,224	**470**
Asturias (*AS*, *Asturias*)	Carbonifer abyssal plain	AS1	0,153	**795**			CU16	0,218	**485**
		AS2	0,158	**755**	*Loza* (*LOZ*, *Alava*)	Eocene lacustrine	LOZ1	0,163	**720**
		AS3	0,114	**1275**			LOZ2	0,161	**735**
Bearn (*BEARN*, *SW France*)	Upper cretaceous abyssal plain	BEAR1	0,158	**755**			LOZ3	0,209	**515**
		BEAR2	0,155	**780**	*Mouguerre* (*MOU*, *SW France*)	Upper cretaceous abyssal plain	MOU2	0,182	**620**
Barrika (*BRK*), *Biscay*	Upper cretaceous abyssal plain	BRK1	0,151	**810**			MOU3	0,187	**595**
		BRK2	0,152	**800**			MOU4	0,172	**670**
		BRK3	0,164	**715**			MOU5	0,176	**650**
		BRK4	0,143	**880**			MOU6	0,183	**615**
San roman (*SR*, *Santander*)	Eocene platform	SR0	0,168	**690**	*Urbasa* (*URB*, *Navarre*)	Paleocene platform	URB7	0,174	**660**
		SR0	0,165	**710**			URB1	0,185	**605**
		SR1	0,180	**630**			URB4	0,187	**595**

way, the crystallite size (in Å) obtained for the analyzed chert samples are summarized in Table 1.

3.2. ATR-IR. Alternative approach for crystal size determination

Particle size modeling can be rather cumbersome though infrared spectra are easily collected. Multivariate calibration techniques, such as partial least squares regression (PLS) have been commonly used to build prediction models in different applications [17–19]. In this case, the possibility to link the infrared spectra and the experimentally measured particle size was tried.

Consequently, once the crystal size of α-quartz was measured by X two different strategies were carried out in order to relate the known crystal size and the IR spectra. In the first strategy, a *soft modeling approach* was followed and it consisted of a multivariate regression of the IR spectra against the known crystal size values. In the second strategy, a *hard modeling approach* was followed since the characteristics of SiO_2 bands of the infrared spectra (i.e. band width, height, etc.) were extracted and those values were linked with the values of the crystal size. In this latter case, multivariate analysis was also used in order to establish this hypothetical link in terms of alterations in stretching or bending vibration modes of SiO_2. Both modeling approaches were performed using The Unscrambler® program (Camo Process AS, Norway, v 7.5).

3.2.1. Soft modeling

The infrared spectra were treated in the absorbance mode and additionally several data treatment alternatives were examined: spectra derivatives and spectra normalization and compared to standardized crystal size used as reference. On the one hand, the derivatives provide sharper bands, especially when shoulders or nonresolved bands are common, and additionally eliminate the shift of the baseline from spectra to spectra. On the other hand, the spectra-wise normalization eliminates the variations that could be attributed to different concentrations or slight differences due to variations in the light path in the ATR-IR measurements and that would be reflected in different intensities in the absorbance.

Based on previous experiences these two data treatments were applied in parallel and without any further standardization of the variables (ATR-IR spectra), that is, Abs. spectra - 1st Derivative - Normalization (ADN) and Abs. spectra - Normalization - 1st Derivative (AND), ending up with two data sets [20,21]. According to a brief analysis of both data sets the second approach (AND) gives slightly better results in terms of the root mean standard error in both calibrations (RMSEC) and prediction (RMSEP), defined as shown in Eqs. (3) and (4). As a consequence all the analysis was carried out taking that data set as target data.

$$RMSEC = \sqrt{\frac{\sum_i (y_{calc} - y_{exp})^2_{calib}}{N}} \tag{3}$$

$$RMSEP = \sqrt{\frac{\sum_i (y_{calc} - y_{exp})^2_{pred}}{N}} \tag{4}$$

The multivariate regression model between the spectra (X) and the experimentally measured crystal size (Y) were built as follows. Firstly, in order to focus on the IR bands of α-quartz, and to eliminate experimental noise and potential interferences we have selected a window between 634 and 1271 cm^{-1}, which means that 661 wavenumbers were taken to generate the prediction model. Regarding the samples, the 65 analyzed samples by means of XRD have been divided in two groups. On the one hand, 37 samples were randomly selected as the training or calibration set and the rest 28 samples were kept as the prediction set. From this latter set, the crystal size of 10 samples was unknown at the time of the prediction.

Based on the training set PLS1 models were built making use of leverage correction as the validation technique and without any scaling of the data. The first models showed some outlying samples (ie., two of the whole data) and samples with a high residual (i.e., another two of the whole data) in the model. Thus, the final prediction model included 33 samples and required 10 PCs (principal components) to explain more than 99% of the variance in the crystal size (*Y*), as shown in Fig. 1a. In the same way, Fig. 1b shows the high agreement between the measured crystal size and the predicted one using the final PLS model (see Table S1).

Based on the final model, the prediction ability was estimated with the prediction set samples. In Fig. 2 the predicted crystal size for validation set of samples and the measured crystal size by means of XRD has been plotted. In order to check the goodness of the PLS model, the accuracy (RMSEP) and precision (as the standard deviation of the predicted crystal size) were also calculated from the experimental values within the prediction data set.

In this sense, the experimental RMSEP value for the PLS model is 165 (Å) whereas the average precision of the estimated size values is roughly 3%. Beyond the quality of the prediction ability, which can be considered adequate in terms of precision but with a significant lack of accuracy, it is not an easy task to understand what is behind this prediction. The calibration models could provide a clue to interpret this regression model after the analysis of the regression parameters values. The significant regression coefficients (higher than 0.1 in absolute values and when *Y* data is scaled) as well as the spectral features that correspond to these regression coefficients are plotted in Fig. 3. When the wavenumbers of the highlighted regression coefficients are compared with the positions of the stretching and bending bands of α-quartz (1160, 1070, 1050, 795, 775, 692 cm^{-1}) it can be suggested that not only the stress on the crystal structure has an effect on the features of the ATR-IR bands but also the crystal size (see Fig. 4).

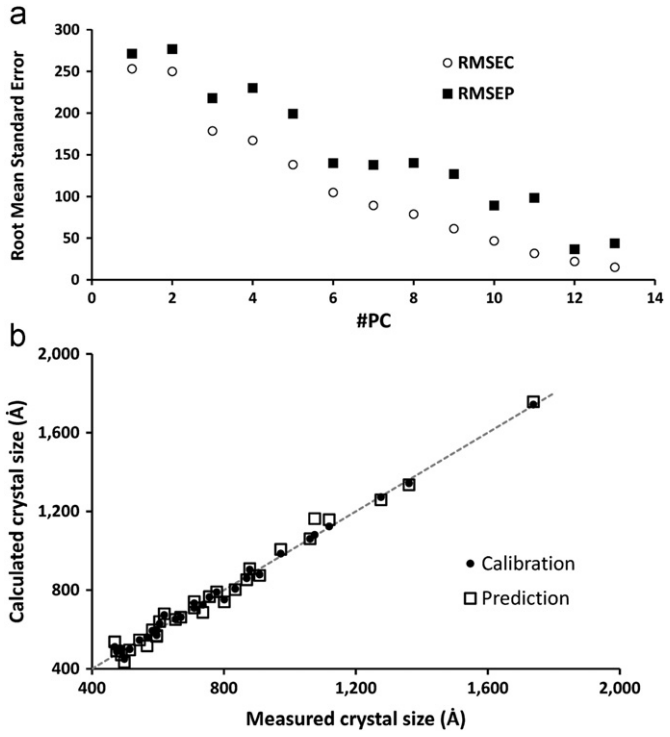

Fig. 1. (a) Root mean standard error of the calibration and prediction against the number of PCs included in the calibration model. (b) Plot of the predicted crystal size against the experimentally measured crystal size values using the first derivate of the normalized infrared spectral data of calibration set.

3.2.2. Hard modeling

This alternative was assayed to give a better background of the IR estimation of crystal size. This strategy meant the integration of the IR bands of SiO_2 between 600 and 1300 cm^{-1} and to extract the band related information such as band height, half maximum width and band area. All these calculations we accomplished using the Grams program (Thermo-Galactic, USA) and the available *curvefit* application.

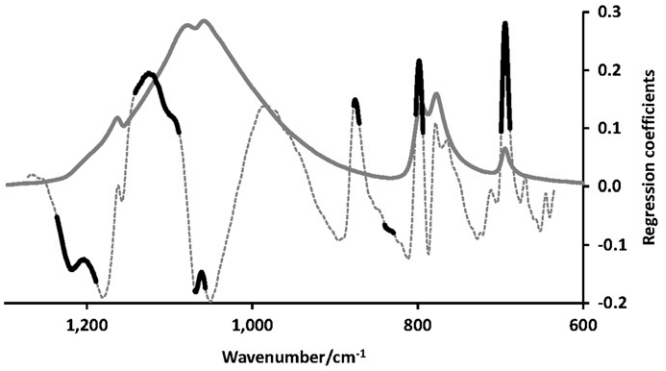

Fig. 3. The infrared spectra in absorbance mode and the significant β-coefficients of the regression model (the highest absolute values ($\beta > 0.1$) are drawn in bold).

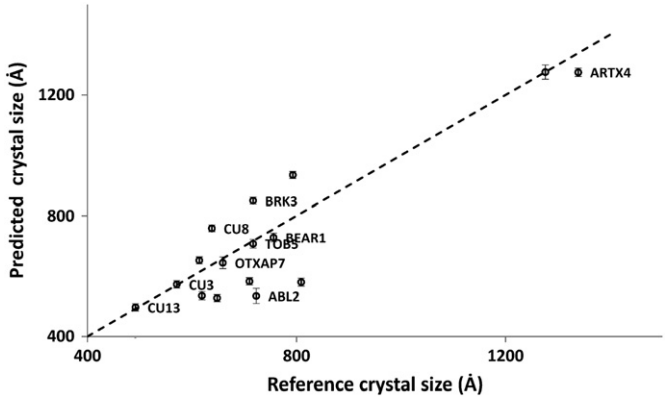

Fig. 2. Plot of the predicted crystal size versus the experimentally measured crystal size values in the prediction set (soft modeling).

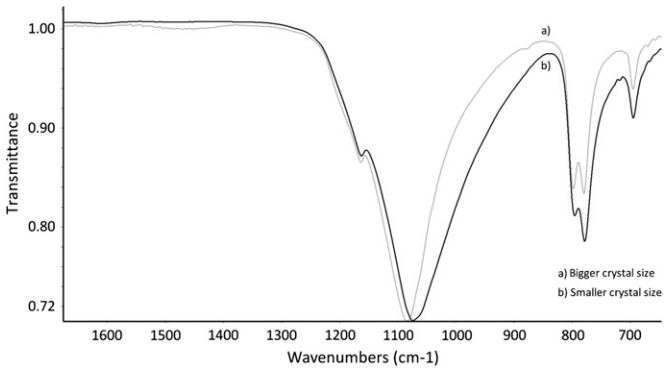

Fig. 4. ATR-IR spectra of two samples with different predicted crystal sizes. (a) ATR-IR spectrum of ABL-1 with bigger crystal size (1124 Å), (b) ATR-IR spectrum of CU-1 with smaller crystal size (619 Å).

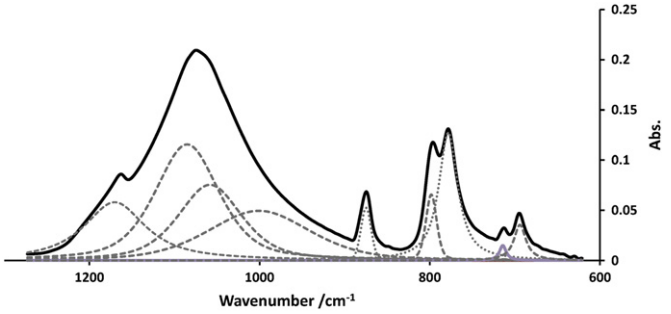

Fig. 5. IR band fitting procedure in CU-6 sample. The raw absorbance spectrum is given with dots and the continuous line corresponds to the curve fitting sum of all the individual bands.

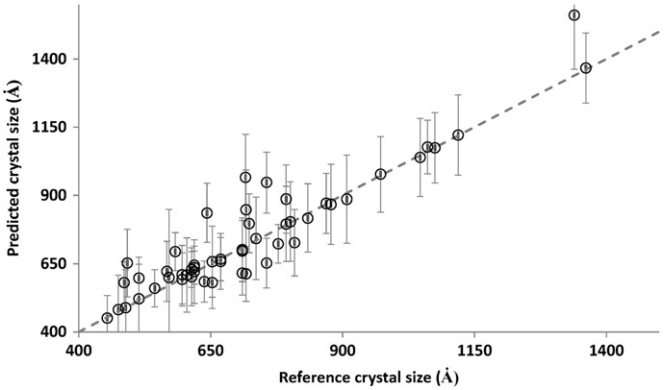

Fig. 6. Plot of the predicted crystal size using the cross validation PLS1 model versus experimentally measured crystal size values using the characteristics of SiO_2 infrared bands (hard modeling).

The deconvolution of the IR bands was carried out according to this general procedure: the baseline was a quadratic function, the bands were a mixture of Gaussian and Lorentzian functions, and a maximum of 50 iterations were done. Although the initial location of the bands can be done automatically, the bands were located manually and the quality of the fit was checked afterwards. Fig. 5 shows the goodness of the overall fitting for one of the deconvoluted signal. Finally band area, width and height of these bands: 1172, 1088, 1059, 799, 779 and 694 cm^{-1}, were collected in one spreadsheet and then transferred to The Unscrambler® program. As it was pointed in the case of soft modeling, from the whole data set, 37 samples were randomly selected from the 65 to be part of the training set.

As expected the raw data table showed that the band height and band area are highly correlated, significantly more correlated than band width and band area. Therefore, although height and area seem to be redundant, all the variables, their interactions and their squared terms were included in the initial regression trials. This calculation was carried out by both PLS1 and MLR (multivariate linear regression) to assure the interpretation of the regression models. In the case of MLR, when all the interactions and squared terms were included, the amount of variables exceeded that of samples and some variables were not finally included.

In the first attempt, scaled variables (X and Y) and leverage correction were the data treatment and the validation scheme respectively and some samples were removed since they were clearly outliers. After that, new calculation was carried out but using cross-validation as the validation scheme in order to identify the most significant variables of each calibration model.

Broadly speaking, band height and band width seem to be the key variables and, on the contrary, band area is systematically less important. Additionally, none of the interactions appeared to be significant, and therefore the models were drastically simplified, and finally, the most valuable variables were the band width and height of the lowest wavenumbers (798, 780 and 694 cm^{-1}) including some squared terms. These conclusions were lately verified by MLR (p-level of regression coefficients < 0.05).

In the two validation schemes, leverage correction and cross-validation, the optimum number of the amount of PCs required was different. In the first case, 13 PCs were required to explain 99% of the total variance whereas the cross validation method gave reasonable good models with less than 10 PCs for the same explained variance. Making use of those two types of models, the prediction step was extended to all the samples. The comparison of the predicted and measured values of crystal size is shown in Fig. 6 (only cross validated model) (see Table S1). The RMSEP value was 80 Å and 100 Å using cross-validation and leverage correction respectively whereas the mean standard deviation was 15% in the case of cross validation and 5% when leverage correction was used.

4. Conclusions

In conclusion, the possibility to estimate the crystal size by means of infrared measurements has been shown by a large amount of measurements. This approach opens new strategies to assess the crystal size by less invasive methods than XRD, being possible to determine this parameter in real valuable samples such as archeological samples. In fact, as a general conclusion, it can be highlighted that the physical stress on the crystal structure has a signature not only in the X-ray diffraction pattern but also in the ATR-IR spectra as well. In the studied case, the variance in the model was associated to the differences in the characteristic stretching and bending infrared bands of SiO_2 which has allowed the prediction of the crystal size. This fact is especially significant in 798, 780 and 694 cm^{-1} bands which are typically attributed to Si–O–Si bending bands of α-quartz. Based on this fact, it would be feasible to estimate the crystal size if a fully validated multivariate model relating the size measured by standard methods and the ATR-IR spectra are available. After the application of the performed soft PLS regression model to the significant part of the ATR-IR spectra, it was possible to predict the crystal size of real chert samples satisfactorily if the experimental root mean standard error of precision value was 165 Å whereas the average precision of the estimated size value was 3%, which is comparable to that obtained by XRD measurements. The accuracy of the predicted crystal size is significantly improved (80 Å) when the hard modeling approach is used, though the precision is much higher (15%).

This new methodology to determine crystal size using non-invasive techniques can be applied to determine the knapping properties of chert samples [3,10]. The crystal size of the studied cherts showed a wide range of variation (i.e. from 450 to 1300 Å) which can allow distinguishing them since the specimens are resilient to greater ranges of temperature variations. This way of doing would mean the comparison of the crystal size in archeological chert samples with that measured in the corresponding geological samples. The variation of the crystal size parameter could be interpreted as a marker of a lithic specimen to describe its quality for knapping purposes in the prehistory as well as to find evidences of thermal treatments.

Acknowledgments

This work was supported by the Research Project CGL2008-00009/BTE and HAR-2008-05797/HIST of the Spanish Ministry of Science

and Innovation. Thanks also to SGIker service from the University of the Basque Country for the performance of XRD analyses.

Appendix A. Supporting information

Supplementary data associated with this article can be found in the online version at http://dx.doi.org/10.1016/j.talanta.2012.06.066.

References

[1] P. Fernandes, J.P. Raynal, M.H. Moncel, J. Archaeol. Sci. 35 (2008) 2357–2370.
[2] V. Lea, Gallia Prehistoire 46 (2004) 231–250.
[3] A. Mercieca, P. Hiscock, J. Archaeol. Sci. 35 (2008) 2634–2639.
[4] M. Martini, E. Sibilia, S. Croci, M. Cremaschi, J. Cult. Heritage 2 (2001) 179–190.
[5] M. Duttine, P. Guilbert, A. Perraut, C. Lahaye, F. Bechtel, G. Villeneuve, Radiat. Meas. 39 (2005) 375–385.
[6] S.A. Ahler, Lithic Technol. 11 (1983) 1–8.
[7] M. Rowney, J.P. White, J. Archaeol. Sci. 24 (1997) 649–657.
[8] R. Joesten, Contact metamorphism, in: D.M. Kerrick (Ed.), Reviews in Mineralogy, vol. 26, Mineralogical Society of America, 1991, pp. 507–582.
[9] J.F. Banfield, H. Zhang, in: J.F. Banfield, A. Navrotsky (Eds.), Nanoparticles and the Environment. Reviews in Mineralogy and Geochemistry, 44, 2001, pp. 1–59.
[10] M. Domanski, J.A. Webb, J. Archaeol. Sci. 19 (1992) 601–614.
[11] P. Schmidth, A. Badon, F. Fröhlich, Spectrochim. Acta A, in press, http://dx.doi.org/10.1016/j.saa.2011.06.050.
[12] P. Schmidth, F. Fröhlich, Spectrochim. Acta A, in press, http://dx.doi.org/10.1016/j.saa.2011.06.036.
[13] P. Schmidth, S. Masse, G. Laurent, A. Slodczyk, E. Le Bourhis, C. Perrenoud, J. Livage, F. Fröhlich, J. Archaeol. Sci. 39 (2012) 135–144.
[14] A. Sharma, D. Prakash, K.D. Verma, J. Optoelectron. Adv. Mater. 11 (2009) 331–337.
[15] W.D. Callister, Material Science and Engineering: An Introduction, 7th ed., John Wiley & Sons, New Jersey, 2000.
[16] J. Martin-Marquez, J.M. Rincon, M. Romero, J. Eur. Ceram. Soc. 30 (2010) 1599–1607.
[17] V.O. Santos Jr., F.C.C. Oliveira, D.G. Lima, A.C. Petry, E. Garcia, P.A.Z. Suarez, J.C. Rubim, Anal. Chim. Acta 547 (2005) 188–196.
[18] K. Meissl, E. Smidt, M. Schwanninger, Talanta 72 (2007) 791–799.
[19] J. Omar, A. Sarmiento, M. Olivares, I. Alonso, N. Etxebarria, J. Raman Spectrosc., in press, http://dx.doi.org/10.1002/jrs.3152.
[20] M. Olivares, N. Etxebarria, G. Arana, K. Castro, X. Murelaga, A. Berreteaga X-Ray Spectrom. 37 (2008) 293–297.
[21] L. Bartolomé, M. Deusto, N. Etxebarria, P. Navarro, A. Usobiaga, O. Zuloaga J. Chromatogr. A 1174 (2007) 40–49.